Chiral partner contribution to sound velocity peak in dense two-color QCD

Mamiya Kawaguchi
Postdoctoral Researcher at University of Chinese Academy of Sciences

M. K., D. Suenaga 2402.00430 [hep-ph]

2024/4/22

Outline

1. Introduction

- Mass-radius relations and sound velocity

2. Sound velocity in 2-color dense QCD

- Similarity/difference between QC_2D and QC_3D
- Lattice observation

3. Effective model analysis in 2-color QCD

- Two color linear sigma model
- Our work in M. K., D. Suenaga arXiv:2402.00430 [hep-ph]

4. Summary

1. Introduction

- Mass-radius relations and sound velocity

Mass-radius relations and QCD

Mass-radius relations of neutron stars

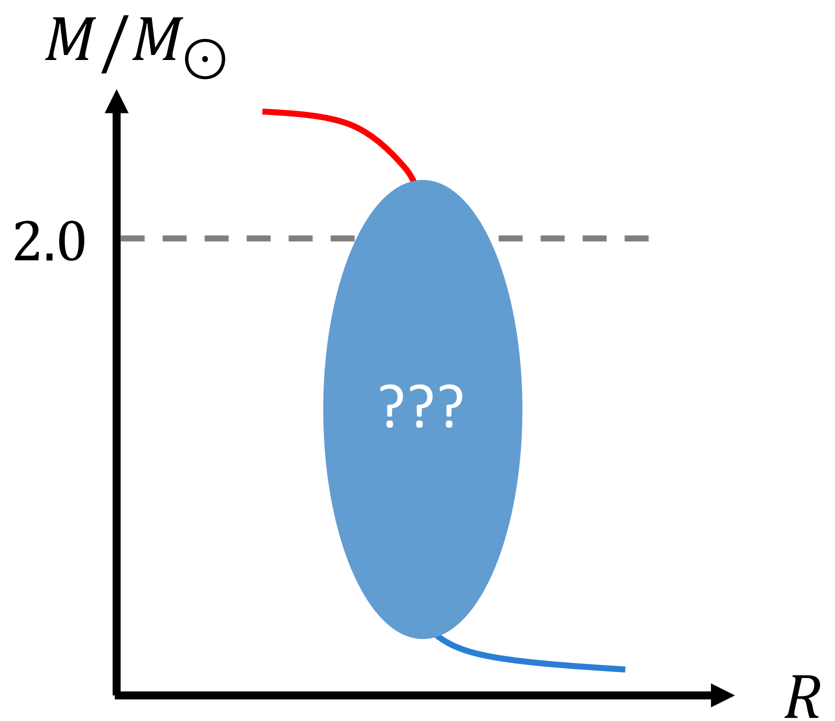

Described by QCD physics

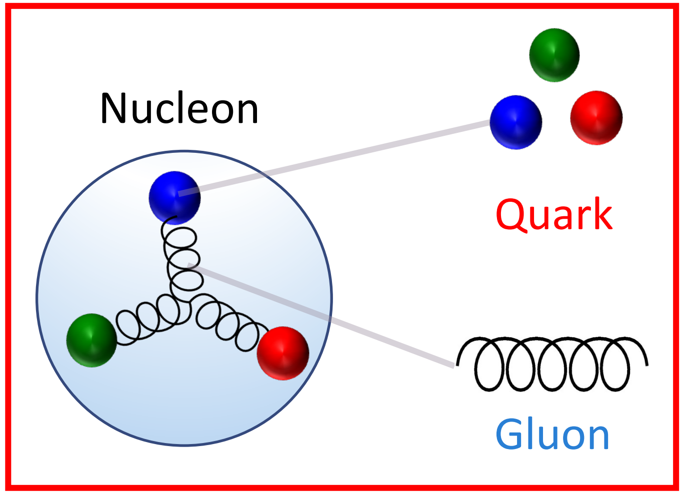

Neutron stars is dense QCD objects.

Mass-radius relations and QCD

Mass-radius relations of neutron stars

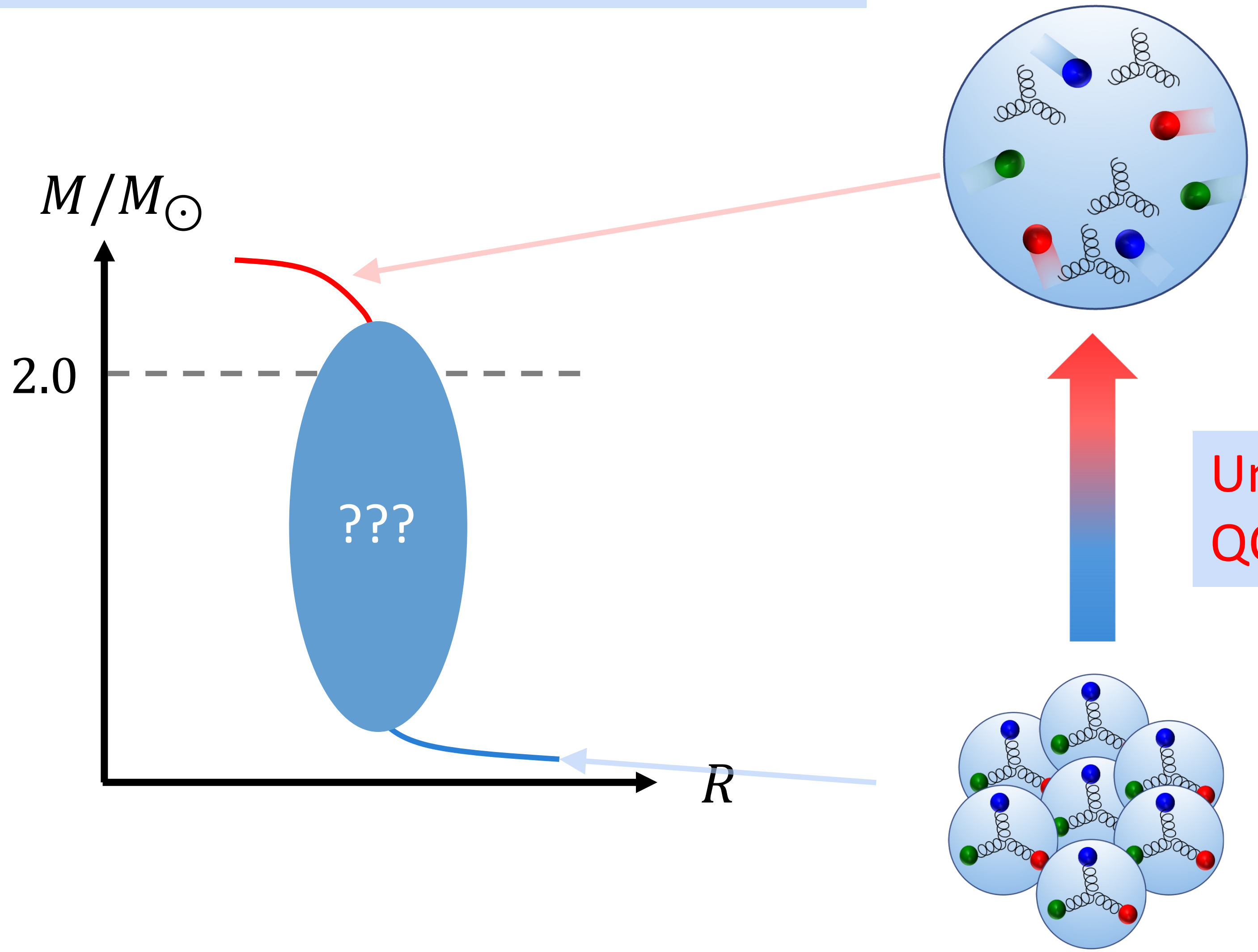

Quark matter

Nuclear matter

Unclear region is closely related to QCD phase transition.

Restriction on energy-pressure relations

Mass-radius relations of neutron stars

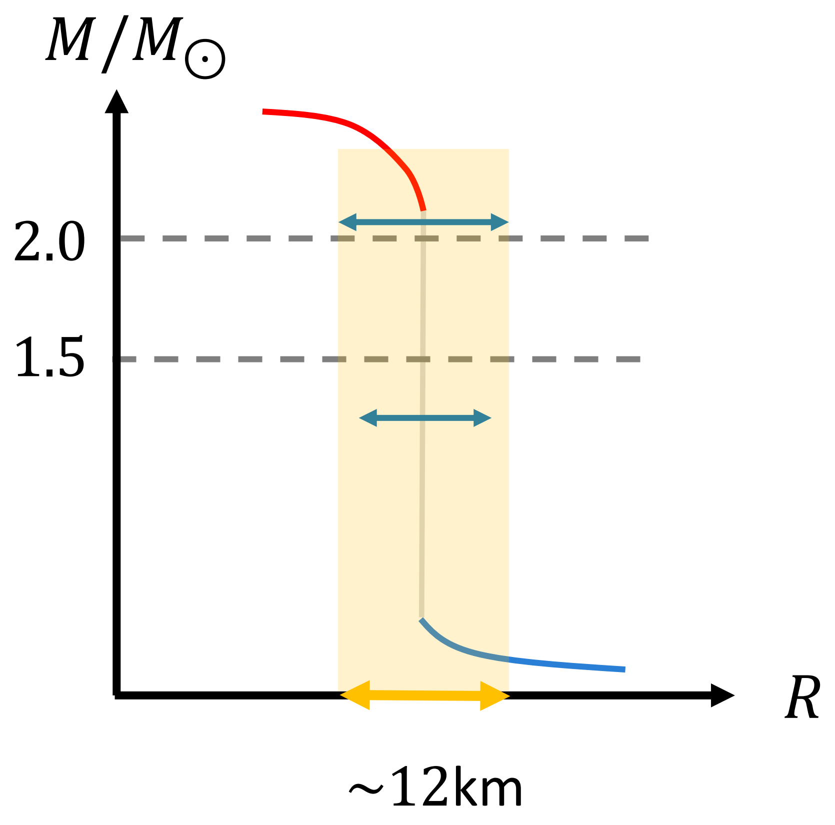

Observations: e.g. M. C. Miller, et al. Astrophys. J. Lett. 918, no.2, L28 (2021)

- 12.35 ± 0.75 km for $2.08 M_\odot$
- 12.45 ± 0.65 km for $1.4\ M_\odot$

Constraint on unclear region.

Energy-pressure relations of neutron stars are also restricted.

Restriction and sound velocity

Energy-pressure relations

Reflected in sound velocity: $c_s^2 = \partial p / \partial \epsilon$

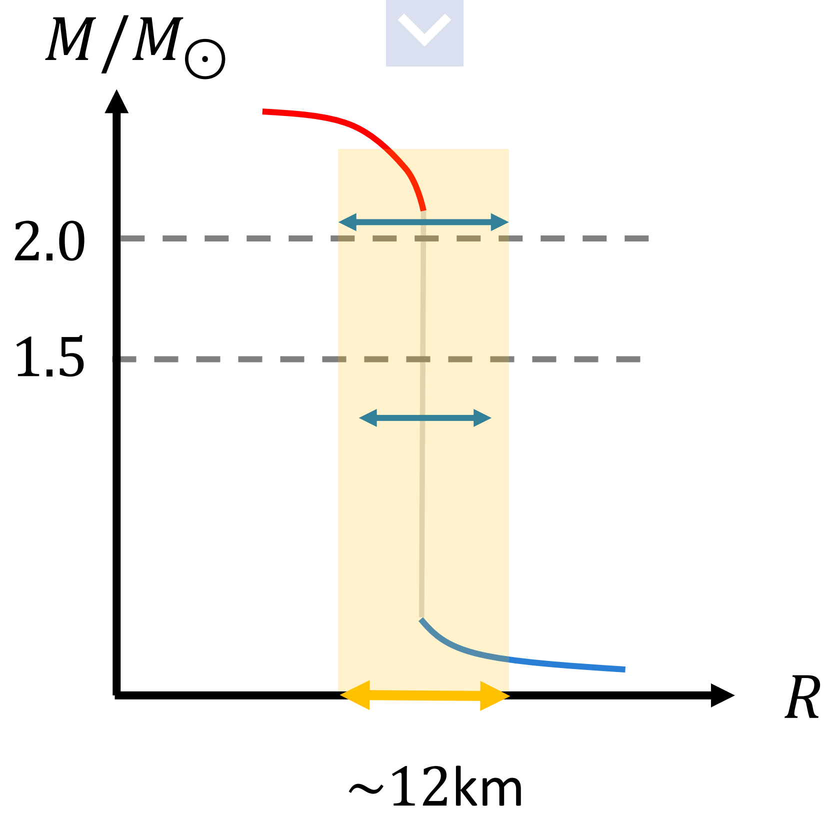

T. Kojo, AAPPS Bull. 31, no.1, 11 (2021)

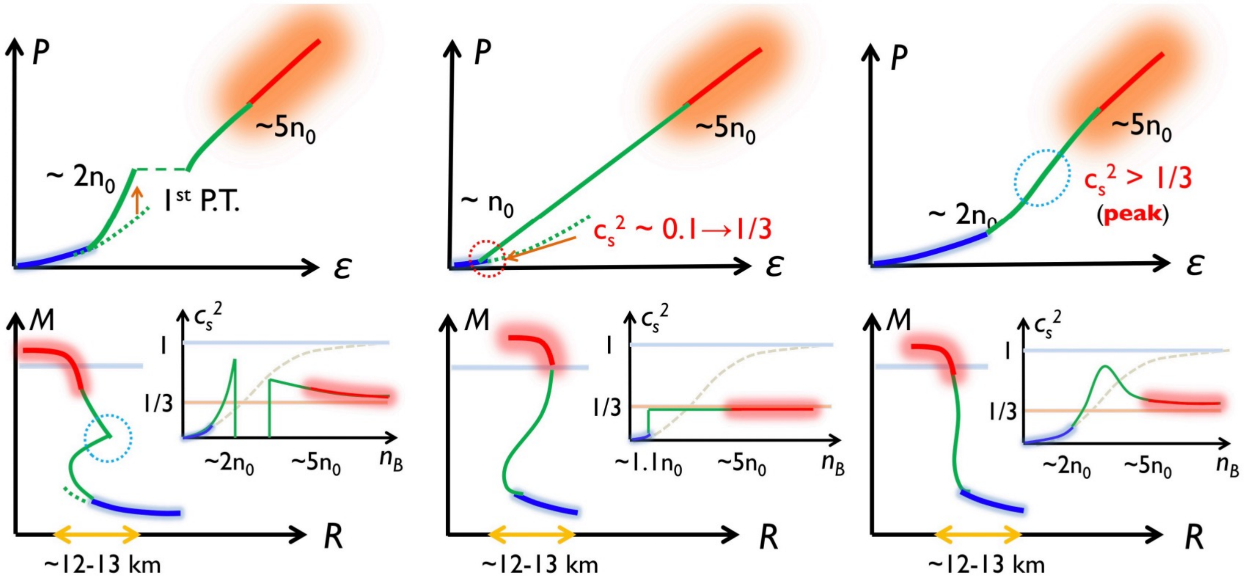

n_0: saturation density of normal nuclear matter

Restriction and sound velocity

Density dependence of sound velocity is essential features.

G. Baym et al., Rept. Prog. Phys. 81, no.5, 056902 (2018)
Y. J. Huang et al., PRL129, no.18, 181101 (2022)

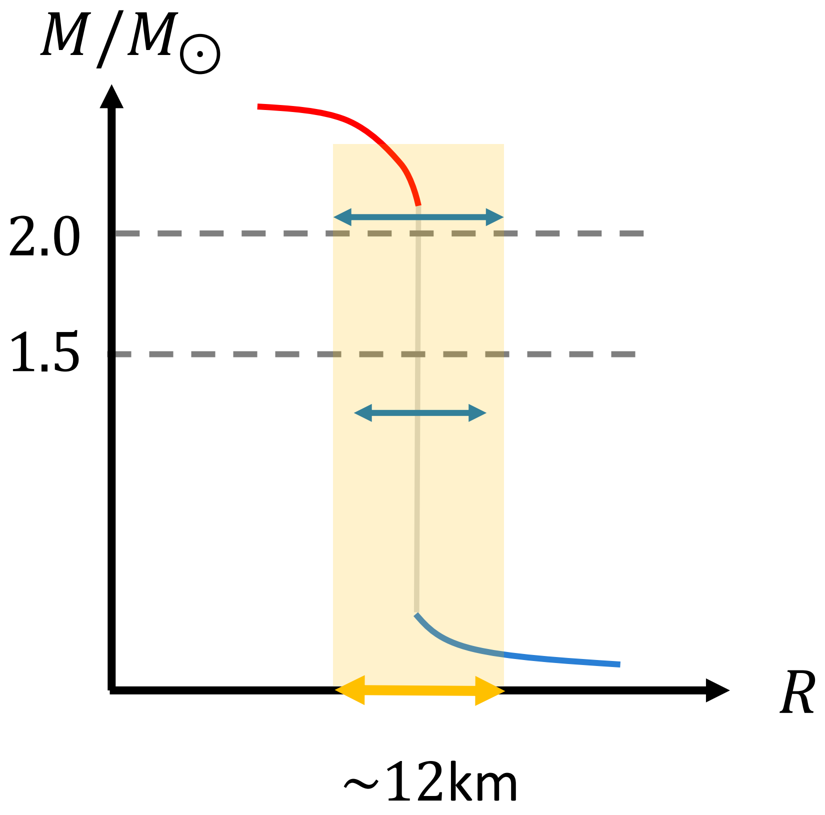

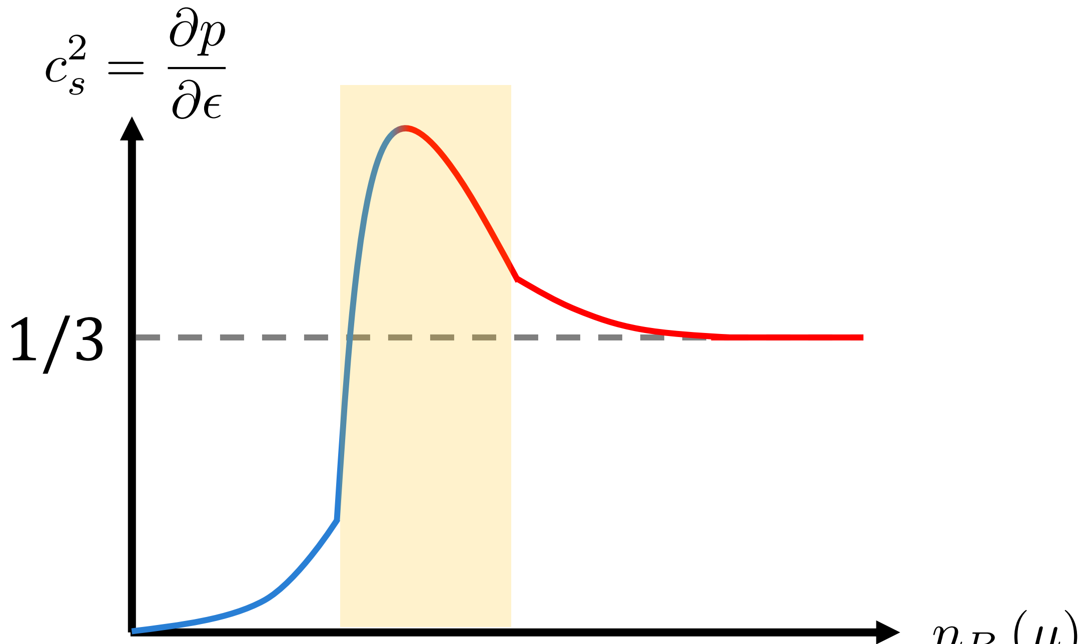

Sound velocity peak provides appropriate mass-radius relations.

Restriction and sound velocity

Density dependence of sound velocity is essential features.

G. Baym et al., Rept. Prog. Phys. 81, no.5, 056902 (2018)
Y. J. Huang et al., PRL129, no.18, 181101 (2022)

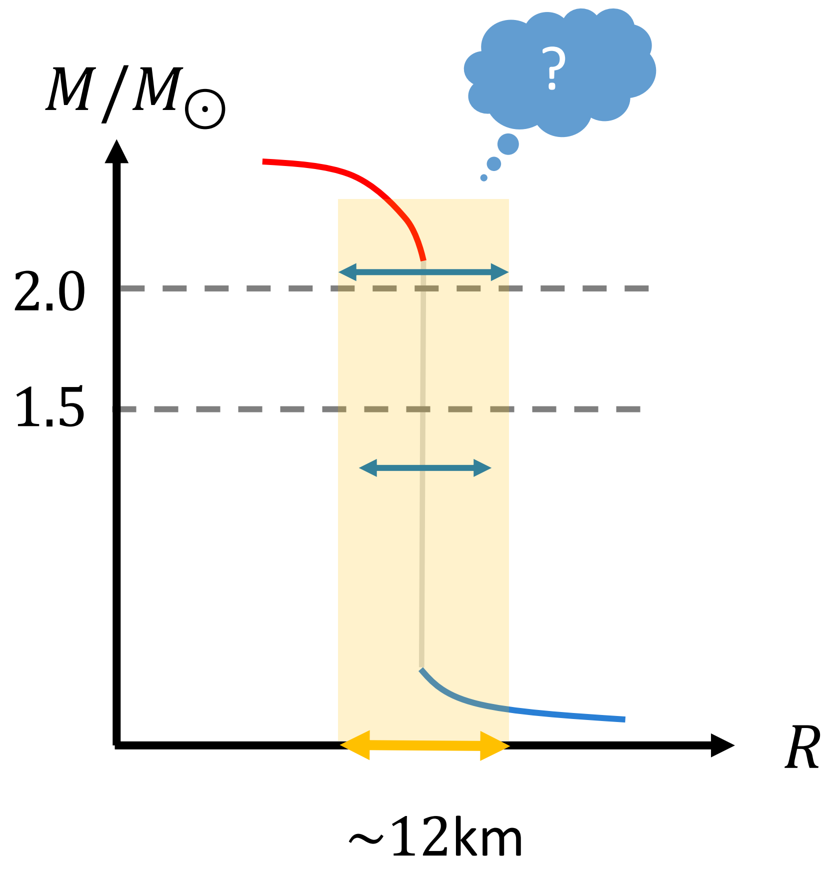

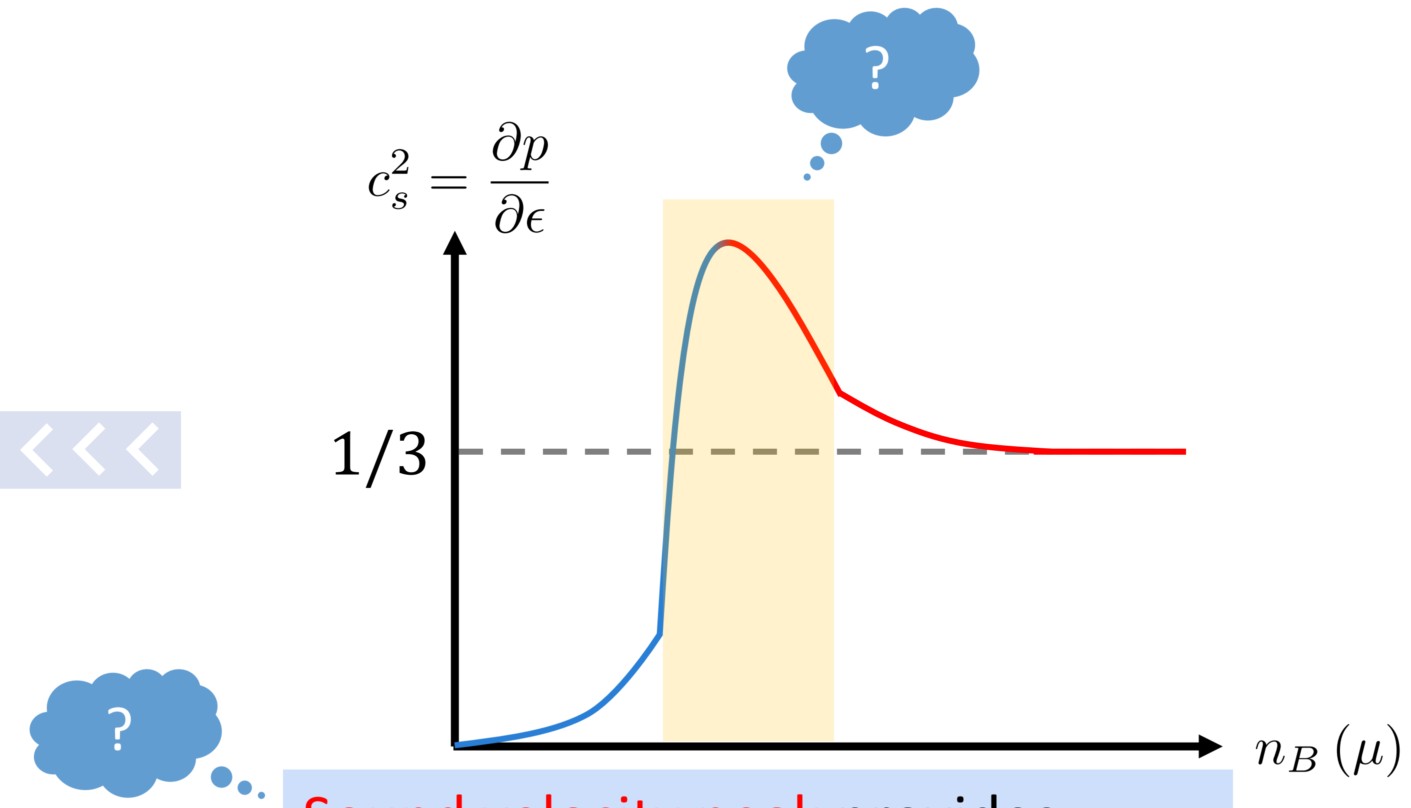

Sound velocity peak provides appropriate mass-radius relations.

Sound velocity and lattice simulation

Peak structure in sound velocity is essential features.

There is growing demand
for first-principle calculations.

QCD lattice simulation

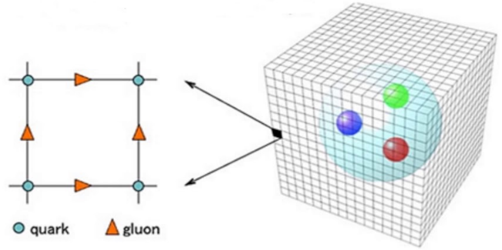

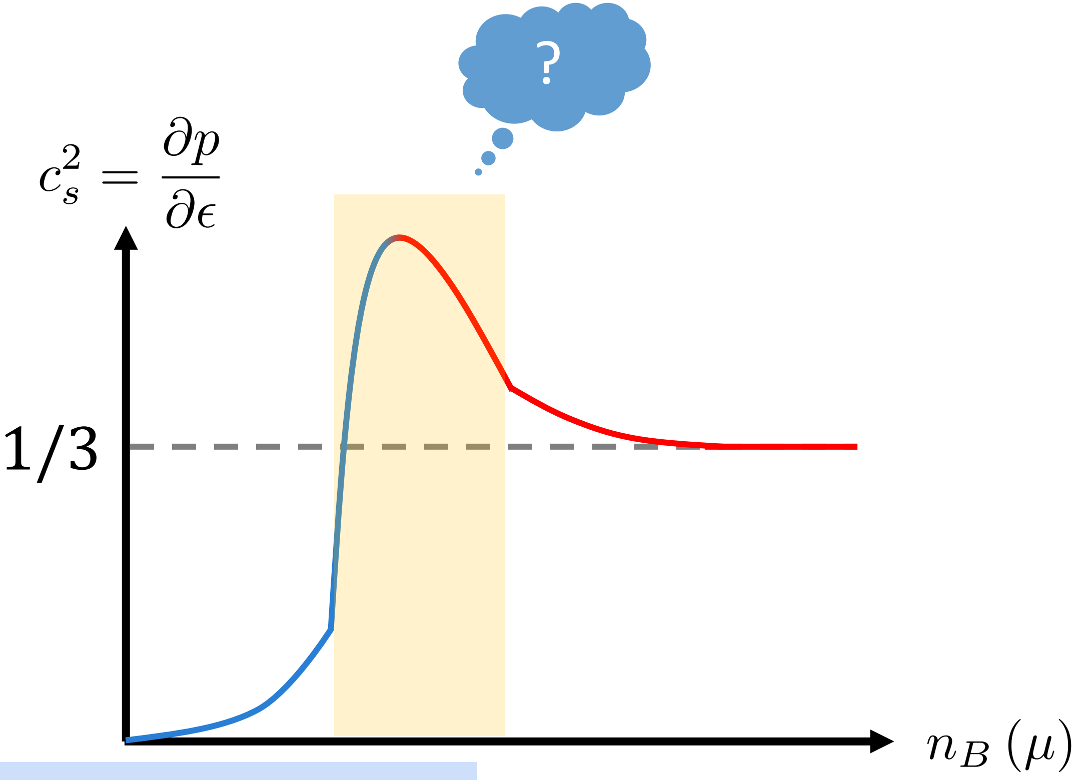

But…

First-principle calculation
cannot be applied to dense system.

This is due to
sign problem.

Sound velocity and lattice simulation

Peak structure in sound velocity is essential features.

We can avoid the sign problem in two-color dense QCD.

Sound velocity has been evaluated in the QC_2D lattice simulation.

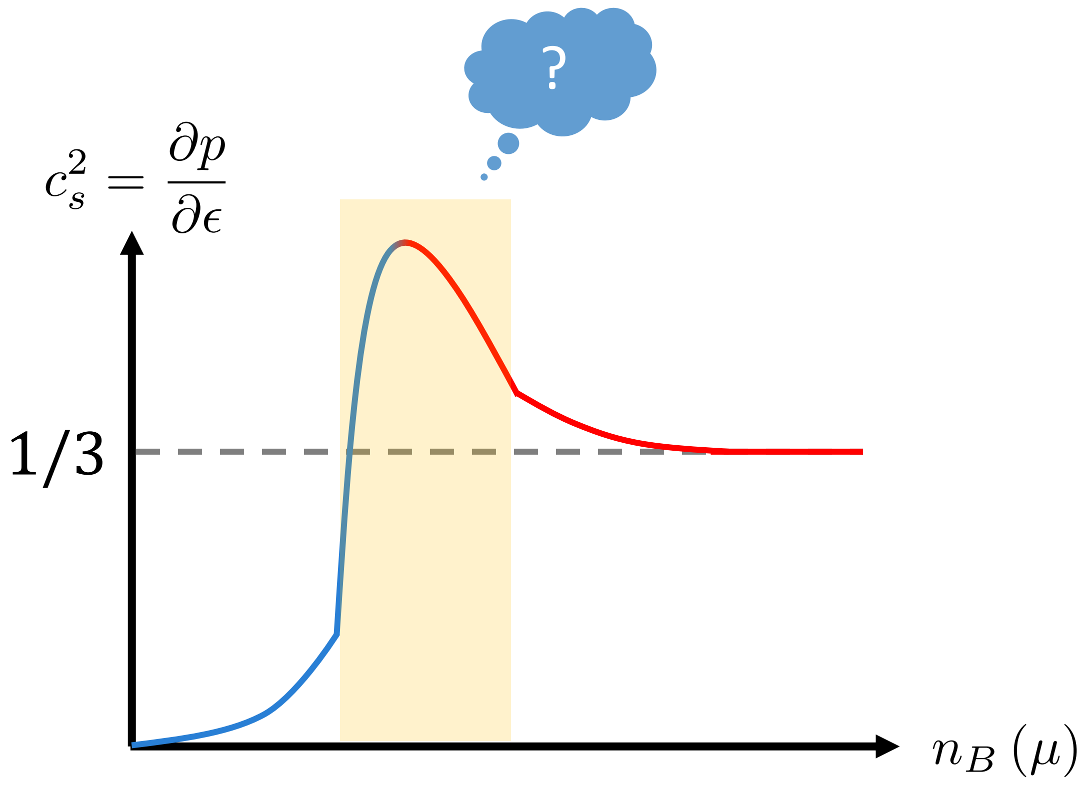

Kei Iida and Etsuko Itou PTEP, 2022(11):111B01, 2022.

2. Sound velocity in 2-color dense QCD

- Similarity/difference between QC_2D and QC_3D
- Lattice observation

Similarity between QC_2D and QC_3D

2-color QCD (QC_2D) system

Quarks are confined, and hadrons are formed.

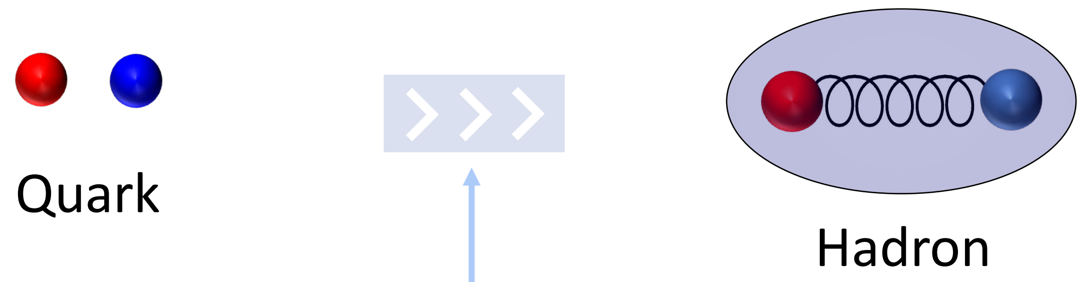

Spontaneous chiral symmetry breaking
also occurs in low energy regime of QC_2D.

"QCD like theory" may be helpful to deepen understanding of "real QCD physics".

Chiral symmetry in dense QC_2D

2-color QCD (QC_2D) system

Quarks are confined, and hadrons are formed.

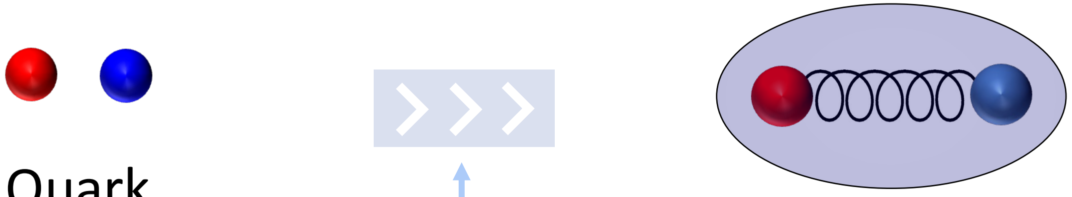

Quark

Hadron

SU(2) has pseudo-real property.

Including μ_q

Sign problem is absent with two flavors.

Spontaneous chiral symmetry breaking
also occurs in low energy regime of QC_2D.

Chiral symmetry in dense QC_2D

2-color QCD (QC_2D) system

Quarks are confined, and hadrons are formed.

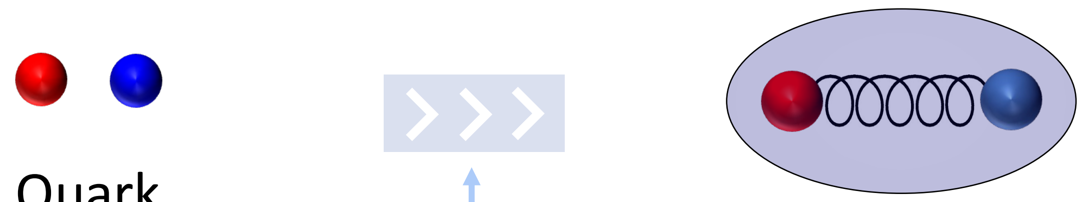

Spontaneous chiral symmetry breaking also occurs in low energy regime of QC_2D.

Density dependence of $\langle \bar{q}q \rangle$

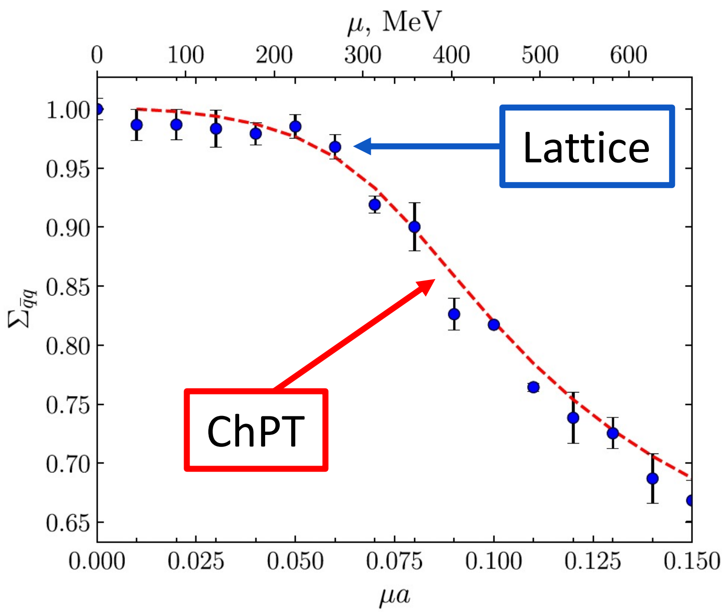

N. Astrakhantsev, et al,
PRD 102, no.7, 074507 (2020)

Chiral symmetry is partially restored.

Difference between QC_2D and QC_3D

3-color QCD

To satisfy the color singlet, baryon consists of three-quarks.

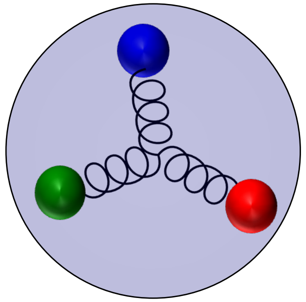

"Fermionic baryon"

2-color QCD

Baryon is formed from two quarks.

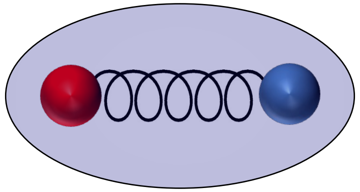

"Bosonic baryon"

Phase transition in dense QC_2D

3-color QCD

To satisfy the color singlet, baryon consists of three-quarks.

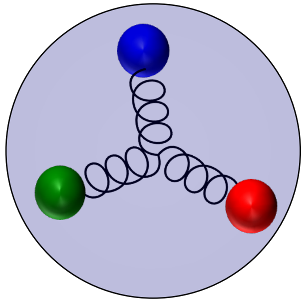

"Fermionic baryon"

2-color QCD

Baryon is formed from two quarks.

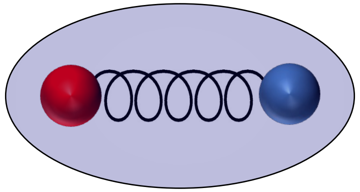

"Bosonic baryon"

Baryon superfluid phase transition

Density dependence of $\langle qq \rangle$

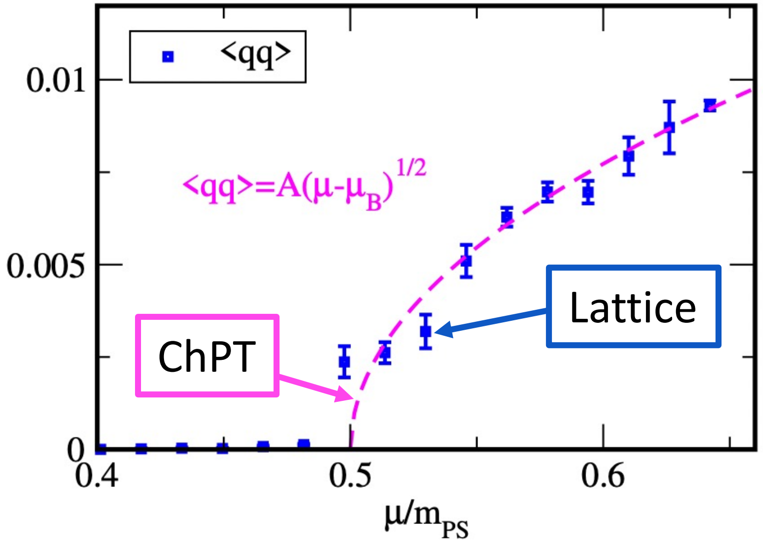

K. Iida, E. Itou and T. G. Lee, JHEP 01, 181 (2020)

QC_2D phase transition occurs in dense system.

2. Sound velocity in 2-color dense QCD

- Similarity/difference between QC_2D and QC_3D
- Lattice observation

Sound velocity in dense QC_2D lattice simulation

Lattice QC_2D observation

Kei Iida and Etsuko Itou PTEP, 2022(11):111B01, 2022.

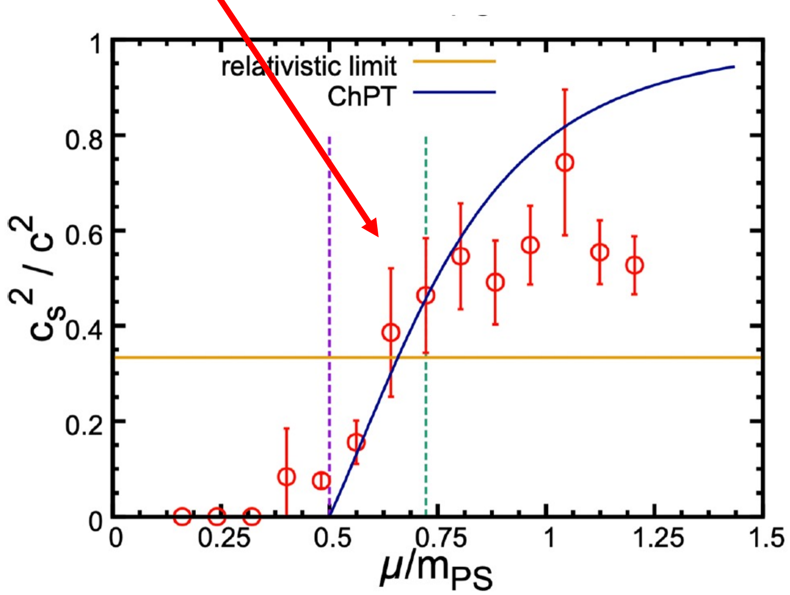

After the phase transition,
it exceeds the conformal limit $c_s^2 = 1/3$.

*At sufficiently large μ (where scale of theory is dominated by only μ: $p \sim \mu^4$), it converges on $c_s^2 = 1/3$.

Appearance of peak structure in QCD-like theory

Sound velocity in dense QC_2D lattice simulation

Lattice QC_2D observation

Kei Iida and Etsuko Itou PTEP, 2022(11):111B01, 2022.

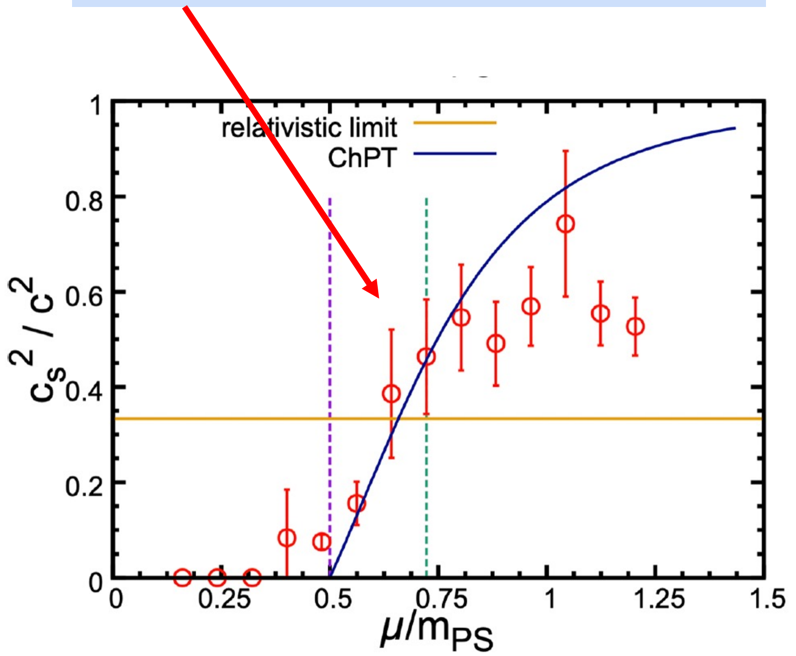

After the phase transition,
it exceeds the conformal limit $c_s^2 = 1/3$.

*At sufficiently large μ (where scale of theory is dominated by only μ: $p \sim \mu^4$),
it converges on $c_s^2 = 1/3$.

Appearance of peak structure in QCD-like theory

May support presence of peak structure in real-life QCD.

QC$_2$D lattice simulation vs ChPT

Lattice QC$_2$D observation

Appearance of peak structure in lattice QC$_2$D

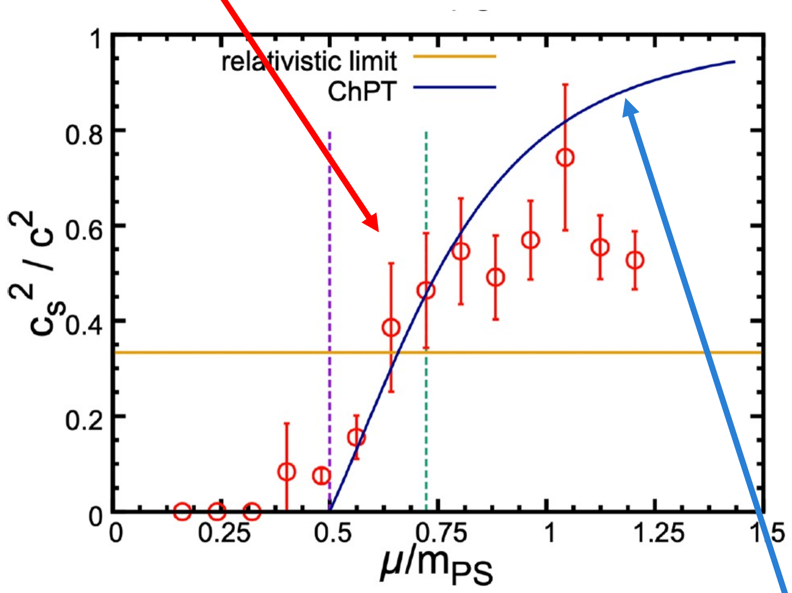

First-principle calculation (Lattice simulation)

?

Discrepancy

Effective model (ChPT)

ChPT result also exceeds the conformal limit $c_s^2 = 1/3$, but converges on $c_s^2 = 1$.

No peak structure in ChPT

Purpose of this study

Address the discrepancy between lattice simulation and effective model.

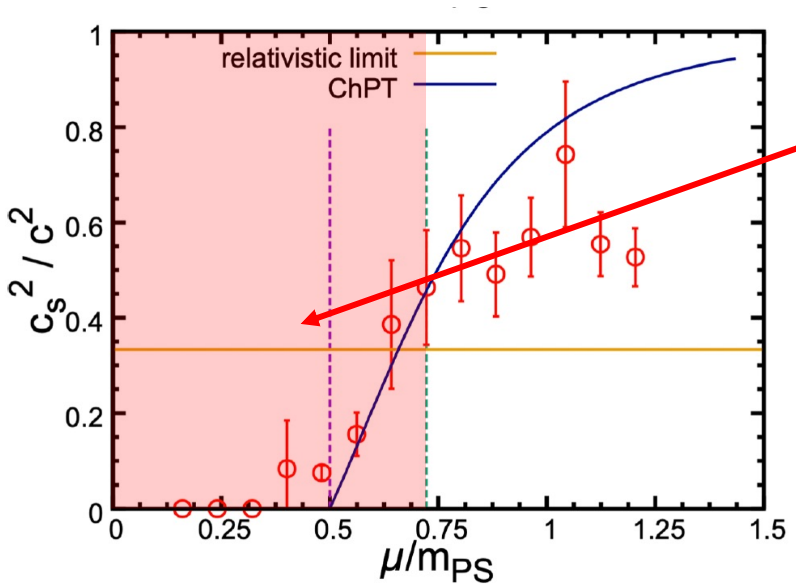

ChPT is adaptable for only the low-energy regime.

(because it is constructed by only Nambu-Goldstone bosons.)

Purpose of this study

Address the discrepancy between lattice simulation and effective model.

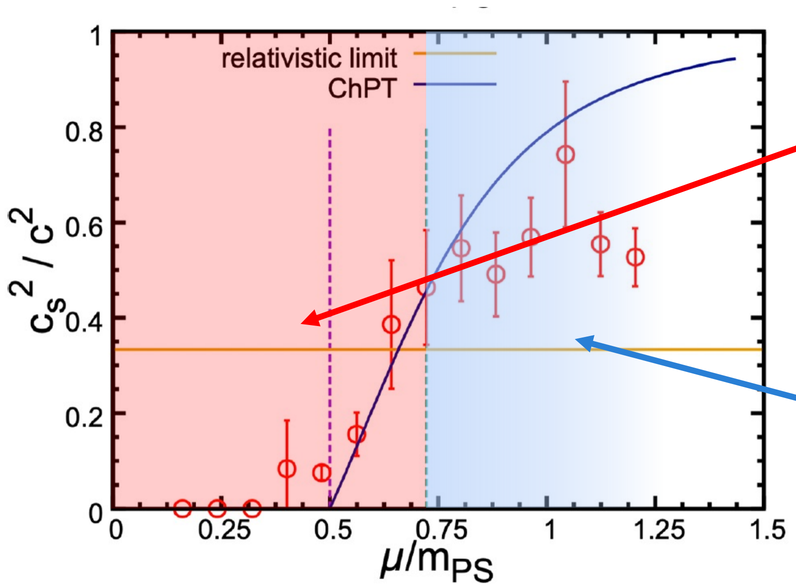

ChPT is adaptable for only the low-energy regime.
(because it is constructed by only Nambu-Goldstone bosons.)

There are overlooked contributions in ChPT.

What contributions provide peak structure?

ChPT and hadron contributions

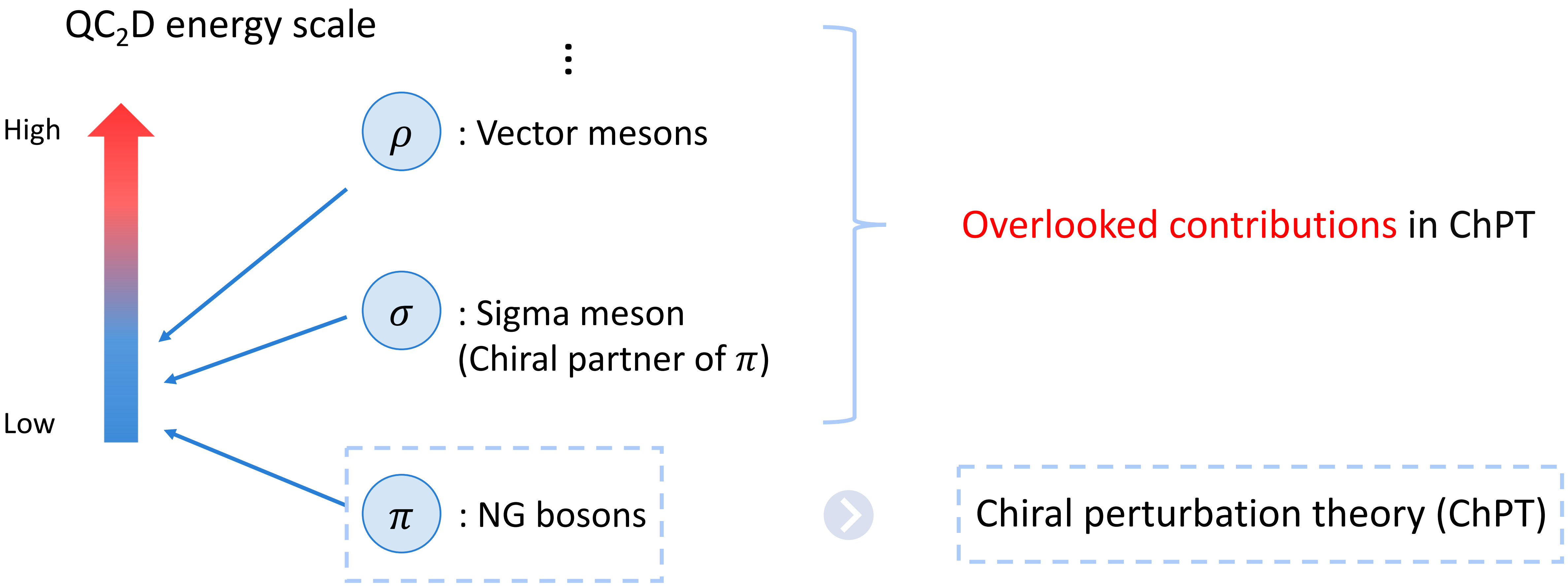

Effective models in QC_2D

QC_2D energy scale

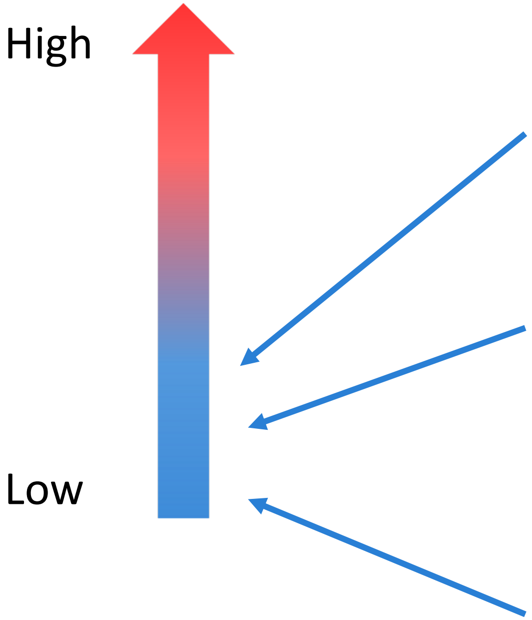

ρ : Vector mesons → **Extended linear sigma model**

D. Suenaga, K. Murakami, E. Itou and K. Iida, [arXiv:2312.17017 [hep-ph]].

σ : Sigma meson (Chiral partner of π) → **Linear sigma model (LSM)**

D. Suenaga, K. Murakami, E. Itou and K. Iida, PRD 107, no.5, 054001 (2023)

π : NG bosons → **Chiral perturbation theory (ChPT)**

Effective model in our study

QC_2D energy scale

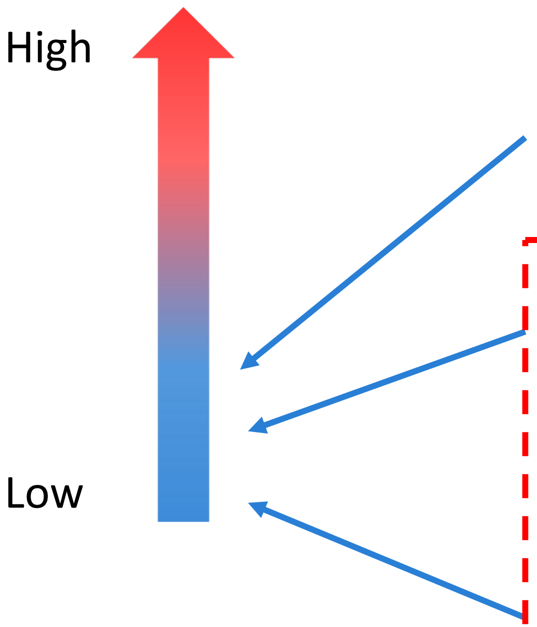

ρ : Vector mesons

σ : Sigma meson (Chiral partner of π)

π : NG bosons

Chiral SU(2) partner

Extended linear sigma model

D. Suenaga, K. Murakami, E. Itou and K. Iida, [arXiv:2312.17017 [hep-ph]].

Linear sigma model (LSM)

D. Suenaga, K. Murakami, E. Itou and K. Iida, PRD 107, no.5, 054001 (2023)

Chiral perturbation theory (ChPT)

In this study, we employ the LSM.

3. Effective model analysis in 2-color QCD

- Two color linear sigma model
- Our work in M. K., D. Suenaga arXiv:2402.00430 [hep-ph]

Effective model of QC_2D at low energy

Linear sigma model
is based on spontaneous chiral symmetry breaking

SU(2) has pseudo-real property.

Including μ_q

Sign problem is absent with two flavors.

Effective model of QC_2D at low energy

Linear sigma model
is based on spontaneous chiral symmetry breaking

π + σ

Building block: $\Sigma = (S^i - i P^i) X^i E$

Chiral symmetry: $\Sigma \rightarrow g\Sigma g^T$

$g \in SU(4)$

- Hadron fields: P^i NG bosons, S^i chiral partners
- X^i: SU(4) generators
- E: symplectic matrix

SU(2) has pseudo-real property.

Including μ_q

Sign problem is absent with two flavors.

- $SU(2)_L \times SU(2)_R$ is extended to $SU(4)$.
- Symmetry breaking pattern: $SU(4) \rightarrow Sp(4)$.
- 5 NG bosons appear.

Effective model of QC_2D at low energy

Linear sigma model
is based on spontaneous chiral symmetry breaking

Building block: $\Sigma = (S^i - i P^i) X^i E$

Chiral symmetry: $\Sigma \to g \Sigma g^T$

$g \in SU(4)$

$$\Sigma = \frac{1}{2} \begin{pmatrix} 0 & -B' + iB & \frac{\sigma - i\eta + a^0 - i\pi^0}{\sqrt{2}} & a^+ - i\pi^+ \\ B' - iB & 0 & a^- - i\pi^- & \frac{\sigma - i\eta - a^0 + i\pi^0}{\sqrt{2}} \\ -\frac{\sigma - i\eta + a^0 - i\pi^0}{\sqrt{2}} & -a^- + i\pi^- & 0 & -\bar{B}' + i\bar{B} \\ -a^+ + i\pi^+ & -\frac{\sigma - i\eta - a^0 + i\pi^0}{\sqrt{2}} & \bar{B}' - i\bar{B} & 0 \end{pmatrix}$$

SU(2) has pseudo-real property.

Including μ_q

Sign problem is absent with two flavors.

Baryon is boson,
which is embedded into Σ.

Effective model of QC_2D at low energy

Linear sigma model
is based on spontaneous chiral symmetry breaking

Building block: $\Sigma = (S^i - i\,P^i)\,X^i\,E$

Chiral symmetry: $\Sigma \to g\Sigma g^T$

$g \in SU(4)$

Chiral invariant Lagrangian:

$$\mathcal{L}_{\mathrm{LSM}} = \mathrm{tr}[D_\mu \Sigma^\dagger D^\mu \Sigma] - V_0 - V_{\mathrm{SB}}$$

- Baryon chemical potential
- Spontaneous symmetry breaking
- Explicit symmetry breaking

- $D_\mu \Sigma = \partial_\mu \Sigma - i\mu_q \delta_{\mu 0}(J\Sigma + \Sigma J^T)$
- $V_0 = m_0^2 \mathrm{tr}[\Sigma^\dagger \Sigma] + \lambda_1 (\mathrm{tr}[\Sigma^\dagger \Sigma])^2 + \lambda_2 \mathrm{tr}[(\Sigma^\dagger \Sigma)^2]$
- $V_{\mathrm{SB}} = -\dfrac{m_l \bar{c}}{2} \mathrm{tr}[E^\dagger \Sigma + \Sigma^\dagger E]$

Effective model of QC_2D at low energy

Linear sigma model
is based on spontaneous chiral symmetry breaking

Building block: $\Sigma = (S^i - i\,P^i)\,X^i\,E$

Chiral symmetry: $\Sigma \to g\Sigma g^T$

$g \in SU(4)$

Chiral invariant Lagrangian:

$$\mathcal{L}_{\rm LSM} = {\rm tr}[D_\mu \Sigma^\dagger D^\mu \Sigma] - V_0 - V_{\rm SB}$$

Mean-field approximation:

$$\langle\Sigma\rangle = (\sigma_0 X_0 - i\Delta X_5)E$$

Sigma meson:
$\sigma_0 = \langle\sigma\rangle \sim \langle\bar{q}q\rangle$

Positive parity baryon:
$\Delta = \langle B\rangle \sim \langle qq\rangle$

Mimics QC_2D phase transition
from hadron phase to baryon superfluid phase.

From LSM to ChPT

Linear sigma model
is based on spontaneous chiral symmetry breaking

Building block: $\Sigma = (S^i - i\, P^i)\, X^i\, E$

Chiral symmetry: $\Sigma \rightarrow g \Sigma g^T$

$g \in SU(4)$

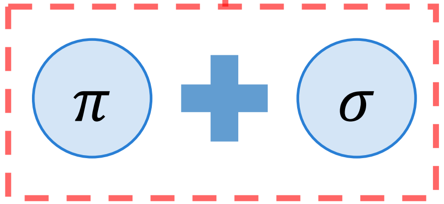

Integrating out chiral partners S^i…

Building block: $\Sigma \sim -f_\pi \mathrm{Exp}\left[i\, P'^i\, X^i\right] E = U$

Chiral symmetry: $\mathrm{U} \rightarrow g U g^T$

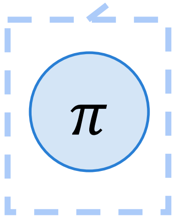

From LSM to ChPT

Linear sigma model
is based on spontaneous chiral symmetry breaking

Building block: $\Sigma = \ (S^i - i\,P^i)\,X^i\,E$

Chiral symmetry: $\Sigma \to g\Sigma g^T$

$g \in SU(4)$

Integrating out
chiral partners S^i...

Building block: $\Sigma \sim -f_\pi \mathrm{Exp}\left[i\,P'^i\,X^i\right]E = U$

Chiral symmetry: U $\to gUg^T$

Chiral perturbation theory (ChPT)

$$\mathcal{L}_{\mathrm{ChPT}} = \frac{f_\pi^2}{4}\mathrm{tr}\left[D_\mu U^\dagger D^\mu U\right] + \frac{f_\pi^2 m_\pi^2}{4}\mathrm{tr}\left[EU + U^\dagger E^\dagger\right]$$

Mean-field approximation:

$$\langle U\rangle = -f_\pi \mathrm{Exp}[i\,\Delta' X^5]E$$

ChPT also provides the phase transition.

3. Effective model analysis in 2-color QCD

- Two color linear sigma model
- Our work in M. K., D. Suenaga arXiv:2402.00430 [hep-ph]

Model results within mean field approximation

ChPT Lagrangian

$$\mathcal{L}_{\mathrm{ChPT}} = \frac{f_\pi^2}{4}\mathrm{tr}\left[D_\mu U^\dagger D^\mu U\right] + \frac{f_\pi^2 m_\pi^2}{4}\mathrm{tr}\left[EU + U^\dagger E^\dagger\right]$$

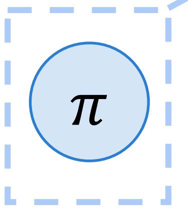

LSM Lagrangian

$$\mathcal{L}_{\mathrm{LSM}} = \mathrm{tr}[D_\mu \Sigma^\dagger D^\mu \Sigma] - m_0^2 \mathrm{tr}[\Sigma^\dagger \Sigma] - \lambda_1 (\mathrm{tr}[\Sigma^\dagger \Sigma])^2 - \lambda_2 \mathrm{tr}[(\Sigma^\dagger \Sigma)^2] + \frac{m_l \bar{c}}{2}\mathrm{tr}[E^\dagger \Sigma + \Sigma^\dagger E]$$

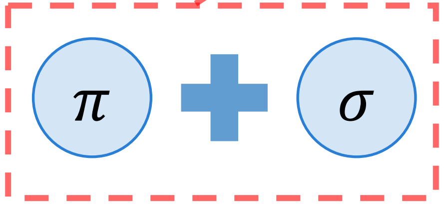

Let's focus on baryonic matter (superfluid phase)

Model results within mean field approximation

ChPT Lagrangian

$$\mathcal{L}_{\rm ChPT} = \frac{f_\pi^2}{4}\mathrm{tr}\left[D_\mu U^\dagger D^\mu U\right] + \frac{f_\pi^2 m_\pi^2}{4}\mathrm{tr}\left[EU + U^\dagger E^\dagger\right]$$

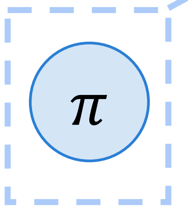

LSM Lagrangian

$$\mathcal{L}_{\rm LSM} = \mathrm{tr}[D_\mu\Sigma^\dagger D^\mu\Sigma] - m_0^2\mathrm{tr}[\Sigma^\dagger\Sigma] - \lambda_1(\mathrm{tr}[\Sigma^\dagger\Sigma])^2 - \lambda_2\mathrm{tr}[(\Sigma^\dagger\Sigma)^2] + \frac{m_l\bar{c}}{2}\mathrm{tr}[E^\dagger\Sigma + \Sigma^\dagger E]$$

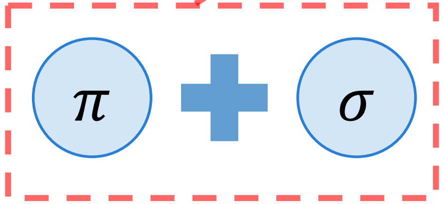

Mean-field approximation:

$$\langle U\rangle = -f_\pi \mathrm{Exp}[i\,\Delta' X^5]E$$

Thermodynamic quantities:

$$p = -V^{\rm mean}$$

$$\epsilon = -p + \mu_q n$$

$$n = \partial p/\partial\mu_q$$

Mean-field approximation:

$$\langle\Sigma\rangle = (\sigma_0 X_0 - i\Delta X_5)E$$

Model results within mean field approximation

ChPT Lagrangian

$$\mathcal{L}_{\rm ChPT} = \frac{f_\pi^2}{4}\mathrm{tr}\left[D_\mu U^\dagger D^\mu U\right] + \frac{f_\pi^2 m_\pi^2}{4}\mathrm{tr}\left[EU + U^\dagger E^\dagger\right]$$

π

$$\bar{\mu} = \mu_q/\mu_q^{\rm cr}$$
$$\mu_q^{\rm cr} = m_\pi/2$$

$$p_{\rm ChPT}^{\rm sub} = f_\pi^2 m_\pi^2 \left(\bar{\mu} - \frac{1}{\bar{\mu}}\right)^2$$

LSM Lagrangian

$$\mathcal{L}_{\rm LSM} = \mathrm{tr}[D_\mu \Sigma^\dagger D^\mu \Sigma] - m_0^2 \mathrm{tr}[\Sigma^\dagger\Sigma] - \lambda_1(\mathrm{tr}[\Sigma^\dagger\Sigma])^2 - \lambda_2 \mathrm{tr}[(\Sigma^\dagger\Sigma)^2] + \frac{m_l \bar{c}}{2}\mathrm{tr}[E^\dagger\Sigma + \Sigma^\dagger E]$$

π + σ

$$\delta\bar{m}_{\sigma-\pi}^2 \equiv \frac{m_\sigma^2 - m_\pi^2}{(\mu_q^{\rm cr})^2}$$

$$p_{\rm LSM}^{\rm sub} = p_{\rm ChPT}^{\rm sub} + f_\pi^2 m_\pi^2 \left[\frac{4}{\delta\bar{m}_{\sigma-\pi}^2}(\bar{\mu}^2 - 1)^2\right]$$

m_π and m_σ are vacuum masses.

Model results within mean field approximation

ChPT Lagrangian

$$\mathcal{L}_{\mathrm{ChPT}} = \frac{f_\pi^2}{4}\mathrm{tr}\left[D_\mu U^\dagger D^\mu U\right] + \frac{f_\pi^2 m_\pi^2}{4}\mathrm{tr}\left[EU + U^\dagger E^\dagger\right]$$

π

$$\bar{\mu} = \mu_q/\mu_q^{\mathrm{cr}}$$

$$\mu_q^{\mathrm{cr}} = m_\pi/2$$

$$p_{\mathrm{ChPT}}^{\mathrm{sub}} = f_\pi^2 m_\pi^2\left(\bar{\mu} - \frac{1}{\bar{\mu}}\right)^2$$

LSM Lagrangian

$$\mathcal{L}_{\mathrm{LSM}} = \mathrm{tr}[D_\mu\Sigma^\dagger D^\mu\Sigma] - m_0^2\mathrm{tr}[\Sigma^\dagger\Sigma] - \lambda_1(\mathrm{tr}[\Sigma^\dagger\Sigma])^2 - \lambda_2\mathrm{tr}[(\Sigma^\dagger\Sigma)^2] + \frac{m_l\bar{c}}{2}\mathrm{tr}[E^\dagger\Sigma + \Sigma^\dagger E]$$

π + σ

Chiral partner contribution

$$\delta\bar{m}_{\sigma-\pi}^2 \equiv \frac{m_\sigma^2 - m_\pi^2}{(\mu_q^{\mathrm{cr}})^2}$$

$$p_{\mathrm{LSM}}^{\mathrm{sub}} = p_{\mathrm{ChPT}}^{\mathrm{sub}} + f_\pi^2 m_\pi^2\left[\frac{4}{\delta\bar{m}_{\sigma-\pi}^2}(\bar{\mu}^2 - 1)^2\right]$$

m_π and m_σ are vacuum masses.

Model results within mean field approximation

ChPT Lagrangian

$$\mathcal{L}_{\mathrm{ChPT}} = \frac{f_\pi^2}{4}\mathrm{tr}\left[D_\mu U^\dagger D^\mu U\right] + \frac{f_\pi^2 m_\pi^2}{4}\mathrm{tr}\left[EU + U^\dagger E^\dagger\right]$$

π

$$\bar{\mu} = \mu_q/\mu_q^{\mathrm{cr}}$$
$$\mu_q^{\mathrm{cr}} = m_\pi/2$$

$$p_{\mathrm{ChPT}}^{\mathrm{sub}} = f_\pi^2 m_\pi^2\left(\bar{\mu} - \frac{1}{\bar{\mu}}\right)^2$$

LSM Lagrangian

$$\mathcal{L}_{\mathrm{LSM}} = \mathrm{tr}[D_\mu \Sigma^\dagger D^\mu \Sigma] - m_0^2 \mathrm{tr}[\Sigma^\dagger\Sigma] - \lambda_1(\mathrm{tr}[\Sigma^\dagger\Sigma])^2 - \lambda_2 \mathrm{tr}[(\Sigma^\dagger\Sigma)^2] + \frac{m_l \bar{c}}{2}\mathrm{tr}[E^\dagger\Sigma + \Sigma^\dagger E]$$

Chiral partner contribution

π + σ

$$\delta\bar{m}_{\sigma-\pi}^2 \equiv \frac{m_\sigma^2 - m_\pi^2}{(\mu_q^{\mathrm{cr}})^2}$$

$$p_{\mathrm{LSM}}^{\mathrm{sub}} = p_{\mathrm{ChPT}}^{\mathrm{sub}} + f_\pi^2 m_\pi^2\left[\frac{4}{\delta\bar{m}_{\sigma-\pi}^2}(\bar{\mu}^2 - 1)^2\right]$$

$$\lim_{m_\sigma\to\infty} p_{\mathrm{LSM}}^{\mathrm{sub}} = p_{\mathrm{ChPT}}^{\mathrm{sub}}$$

LSM result is beyond lowest energy regime.

Sound velocity within mean field approximation

ChPT Lagrangian

π

$$\bar{\mu} = \mu_q / \mu_q^{\rm cr}$$
$$\mu_q^{\rm cr} = m_\pi / 2$$

$$p_{\rm ChPT}^{\rm sub} = f_\pi^2 m_\pi^2 \left(\bar{\mu} - \frac{1}{\bar{\mu}} \right)^2$$

$$\left(c_s^{\rm ChPT}\right)^2 = \frac{1 - 1/\bar{\mu}^4}{1 + 3/\bar{\mu}^4}$$

S. Hands, S. Kim and J. I. Skullerud, EPJC 48, 193 (2006)

LSM Lagrangian

Chiral partner contribution

π + σ

$$\delta \bar{m}_{\sigma-\pi}^2 \equiv \frac{m_\sigma^2 - m_\pi^2}{(\mu_q^{\rm cr})^2}$$

$$p_{\rm LSM}^{\rm sub} = p_{\rm ChPT}^{\rm sub} + f_\pi^2 m_\pi^2 \left[\frac{4}{\delta \bar{m}_{\sigma-\pi}^2} (\bar{\mu}^2 - 1)^2 \right]$$

$$\left(c_s^{\rm LSM}\right)^2 = \frac{(1 - 1/\bar{\mu}^4) + 8(\bar{\mu}^2 - 1)/\delta \bar{m}_{\sigma-\pi}^2}{(1 + 3/\bar{\mu}^4) + 8(3\bar{\mu}^2 - 1)/\delta \bar{m}_{\sigma-\pi}^2},$$

M. K., D. Suenaga arXiv:2402.00430 [hep-ph]

Sound velocity in LSM at high density regions

M. K., D. Suenaga arXiv:2402.00430 [hep-ph]

Sound velocity in LSM

$$\left(c_s^{\mathrm{LSM}}\right)^2 = \frac{(1-1/\bar{\mu}^4) + 8(\bar{\mu}^2-1)/\delta\bar{m}_{\sigma-\pi}^2}{(1+3/\bar{\mu}^4) + 8(3\bar{\mu}^2-1)/\delta\bar{m}_{\sigma-\pi}^2},$$

- High density regions: $(\mu \gg \mu_{cr})$

$$\left(c_s^{\mathrm{LSM}}\right)^2 = \frac{1}{3} + \frac{\delta\bar{m}_{\sigma-\pi}^2 - 8}{36}\frac{1}{\bar{\mu}^2} + \mathcal{O}\left(1/\bar{\mu}^3\right)$$

In contrast to ChPT, LSM converges on $c_s^2 = 1/3$.

Sound velocity in LSM at high density regions

M. K., D. Suenaga arXiv:2402.00430 [hep-ph]

Sound velocity in LSM

$$\left(c_s^{\rm LSM}\right)^2 = \frac{(1-1/\bar{\mu}^4)+8(\bar{\mu}^2-1)/\delta\bar{m}^2_{\sigma-\pi}}{(1+3/\bar{\mu}^4)+8(3\bar{\mu}^2-1)/\delta\bar{m}^2_{\sigma-\pi}},$$

- High density regions: $(\mu \gg \mu_{cr})$

$$\left(c_s^{\rm LSM}\right)^2 = \frac{1}{3} + \frac{\delta\bar{m}^2_{\sigma-\pi}-8}{36}\frac{1}{\bar{\mu}^2} + \mathcal{O}\left(1/\bar{\mu}^3\right)$$

In contrast to ChPT, LSM converges on $c_s^2 = 1/3$.

For $\delta\overline{m}^2_{\sigma-\pi} \leq 8$ $\left(m_\sigma \leq \sqrt{3}m_\pi\right)$, converges on $c_s^2 = 1/3$ from below.

For $\delta\overline{m}^2_{\sigma-\pi} > 8$ $\left(m_\sigma > \sqrt{3}m_\pi\right)$, converges on $c_s^2 = 1/3$ from above.

Peak in LSM and constraint

M. K., D. Suenaga arXiv:2402.00430 [hep-ph]

Sound velocity in LSM

$$\left(c_s^{\rm LSM}\right)^2 = \frac{(1-1/\bar{\mu}^4)+8(\bar{\mu}^2-1)/\delta\bar{m}^2_{\sigma-\pi}}{(1+3/\bar{\mu}^4)+8(3\bar{\mu}^2-1)/\delta\bar{m}^2_{\sigma-\pi}},$$

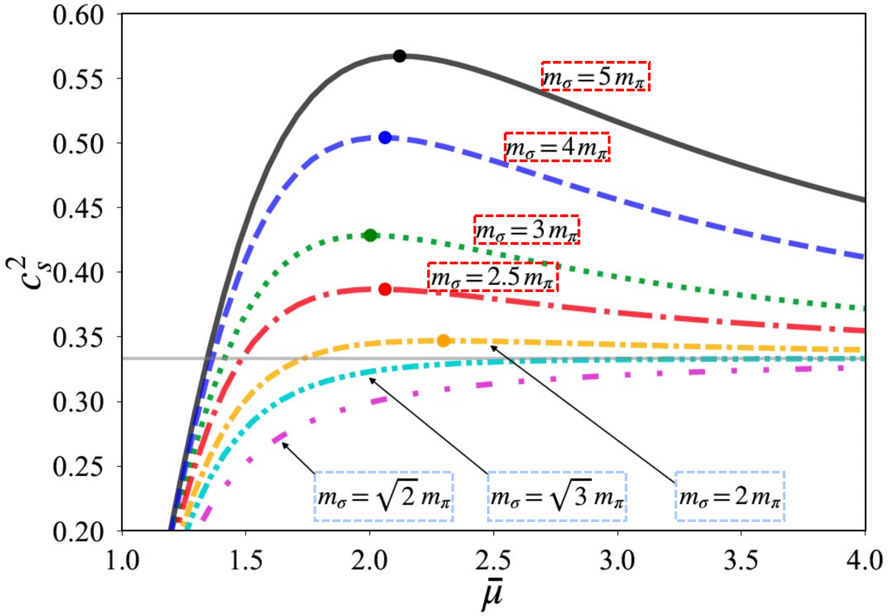

$\bar{\mu} = \mu_q/\mu_q^{\rm cr}$

For $\delta\bar{m}^2_{\sigma-\pi} > 8$ $\left(m_\sigma > \sqrt{3}m_\pi\right)$,

Converges on $c_s^2 = 1/3$ from above.

Appearance of peak

For $\delta\bar{m}^2_{\sigma-\pi} \leq 8$ $\left(m_\sigma \leq \sqrt{3}m_\pi\right)$

Converges on $c_s^2 = 1/3$ from below.

No peak structure

More constraint

M. K., D. Suenaga arXiv:2402.00430 [hep-ph]

Sound velocity in LSM

$$\left(c_s^{\rm LSM}\right)^2 = \frac{(1-1/\bar{\mu}^4)+8(\bar{\mu}^2-1)/\delta\bar{m}^2_{\sigma-\pi}}{(1+3/\bar{\mu}^4)+8(3\bar{\mu}^2-1)/\delta\bar{m}^2_{\sigma-\pi}},$$

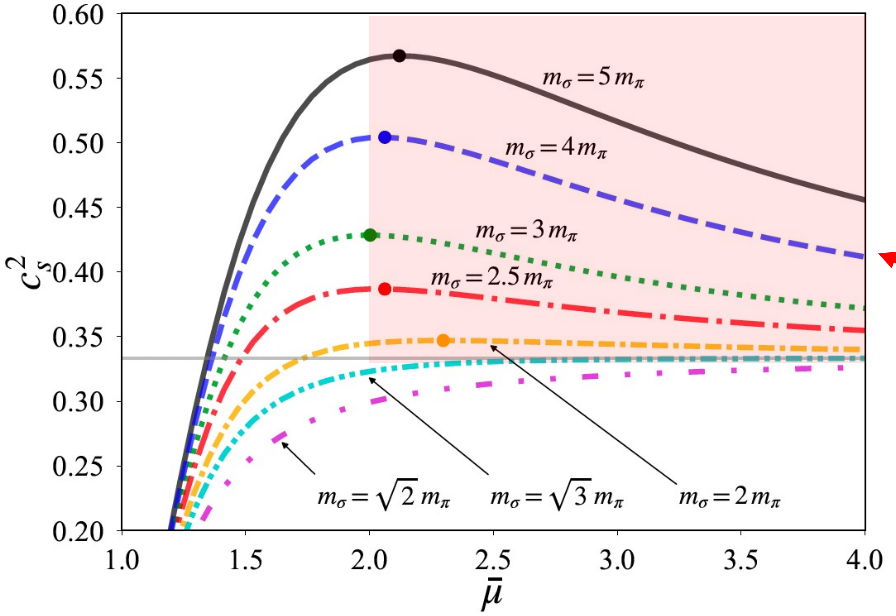

$\bar{\mu} = \mu_q/\mu_q^{\rm cr}$

For $\delta\bar{m}^2_{\sigma-\pi} > 8$ $\left(m_\sigma > \sqrt{3}m_\pi\right)$,

Converges on $c_s^2 = 1/3$ from above.

Appearance of peak

Peak position is only allowed for $\mu > m_\pi$.

Peak structure is induced by chiral partner.

μ dependence of trace anomaly

Lattice QC_2D observation

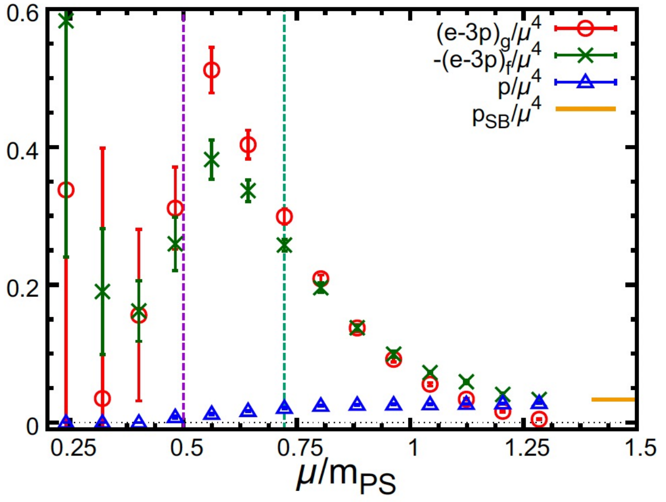

Kei Iida and Etsuko Itou PTEP, 2022(11):111B01, 2022.

μ dependence of trace anomaly has also been observed.
It becomes negative in high-density regions.

μ dependence of trace anomaly

Lattice QC_2D observation

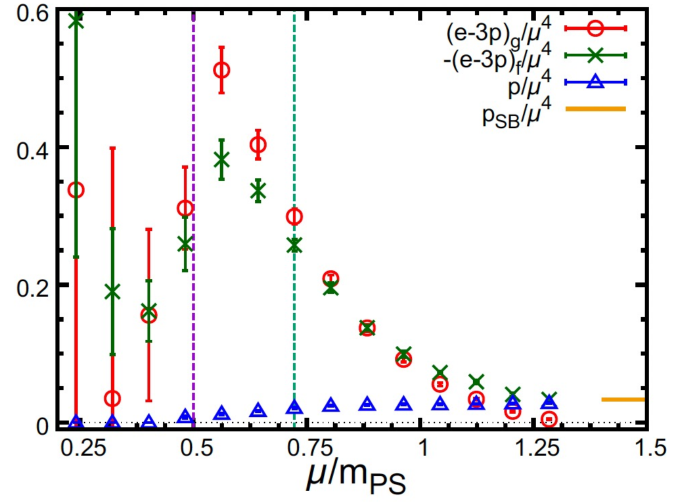

Kei Iida and Etsuko Itou PTEP, 2022(11):111B01, 2022.

μ dependence of trace anomaly has also been observed.
It becomes negative in high-density regions.

LSM evaluation

Chiral partner contribution

$$(\Theta^{\rm sub}_{\rm LSM})^{\mu}_{\mu} = \epsilon^{\rm sub}_{\rm LSM} - 3p^{\rm sub}_{\rm LSM} = (\Theta_{\rm ChPT})^{\mu}_{\mu} + \delta\Theta^{\mu}_{\mu},$$

$$\delta\Theta^{\mu}_{\mu} \propto 1/\delta\bar{m}^2_{\sigma-\pi}$$

$$\delta\bar{m}^2_{\sigma-\pi} \equiv \frac{m_\sigma^2 - m_\pi^2}{(\mu_q^{\rm cr})^2}$$

μ dependence of trace anomaly

Lattice QC_2D observation

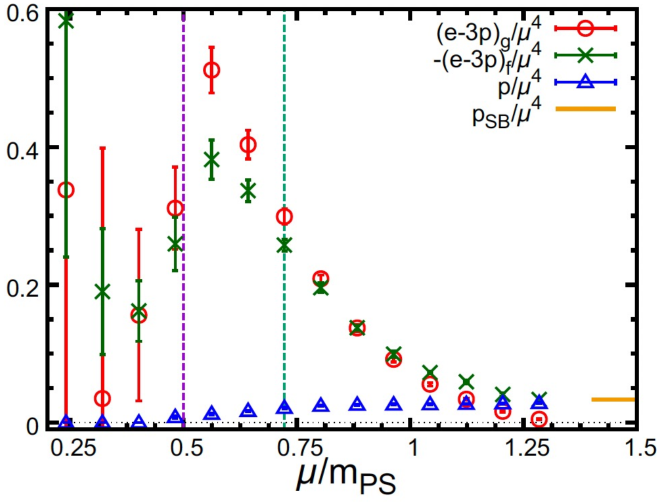

Kei Iida and Etsuko Itou PTEP, 2022(11):111B01, 2022.

μ dependence of trace anomaly has also been observed.
It becomes negative in high-density regions.

LSM evaluation

$$(\Theta^{\rm sub}_{\rm LSM})^{\mu}_{\mu} = \epsilon^{\rm sub}_{\rm LSM} - 3p^{\rm sub}_{\rm LSM}$$
$$= (\Theta_{\rm ChPT})^{\mu}_{\mu} + \delta\Theta^{\mu}_{\mu},$$

$$\delta\Theta^{\mu}_{\mu} \propto 1/\delta\bar{m}^2_{\sigma-\pi}$$

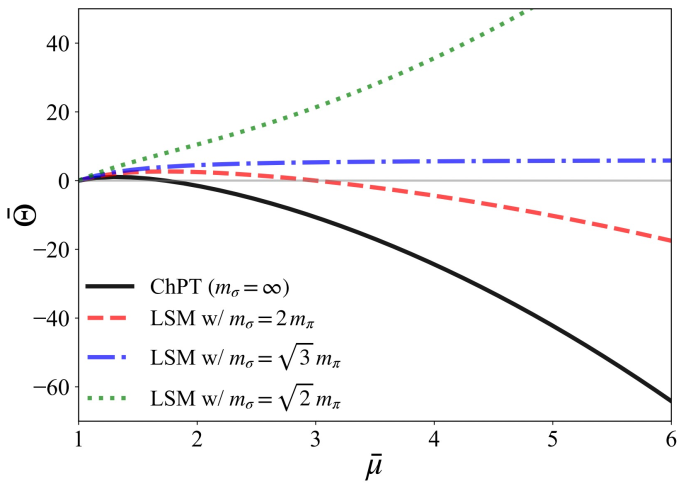

For $m_\sigma > \sqrt{3}m_\pi$,
appearance of peak in c_s^2
and negative trace anomaly

M. K., D. Suenaga arXiv:2402.00430 [hep-ph]

For $m_\sigma \leq \sqrt{3}m_\pi$,
no peak structure in c_s^2
and positive trace anomaly

4. Summary

Summary

M. K., D. Suenaga arXiv:2402.00430 [hep-ph]

What contributions provide peak structure?

$$\delta\bar{m}^2_{\sigma-\pi} \equiv \frac{m_\sigma^2 - m_\pi^2}{(\mu_q^{\rm cr})^2}$$

QC$_2$D energy scale

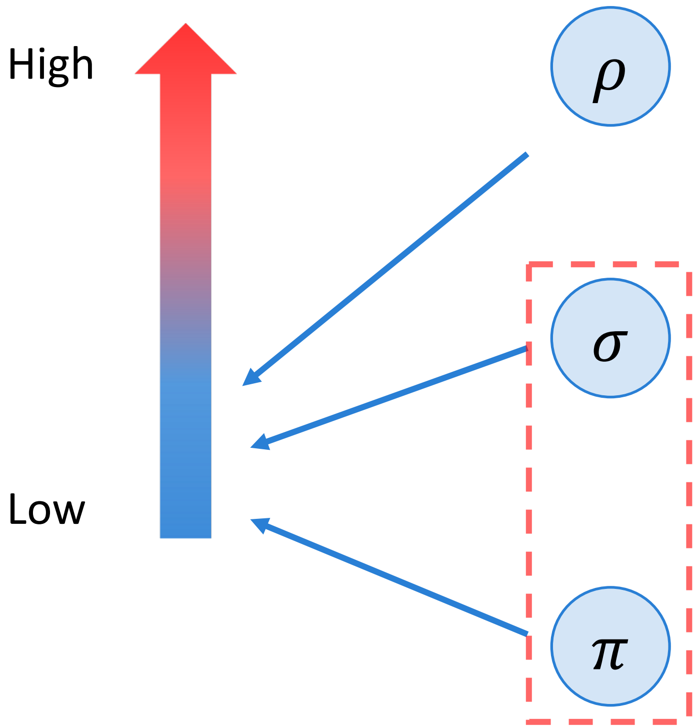

Chiral partner is significant.

Sound velocity in LSM

$$\left(c_s^{\rm LSM}\right)^2 = \frac{(1-1/\bar{\mu}^4) + 8(\bar{\mu}^2-1)/\delta\bar{m}^2_{\sigma-\pi}}{(1+3/\bar{\mu}^4) + 8(3\bar{\mu}^2-1)/\delta\bar{m}^2_{\sigma-\pi}},$$

For $m_\sigma > \sqrt{3}m_\pi$,

- peak appears in c_s^2 for $\mu > m_\pi$.
- trace anomaly becomes negative.

Summary

M. K., D. Suenaga arXiv:2402.00430 [hep-ph]

What contributions provide peak structure?

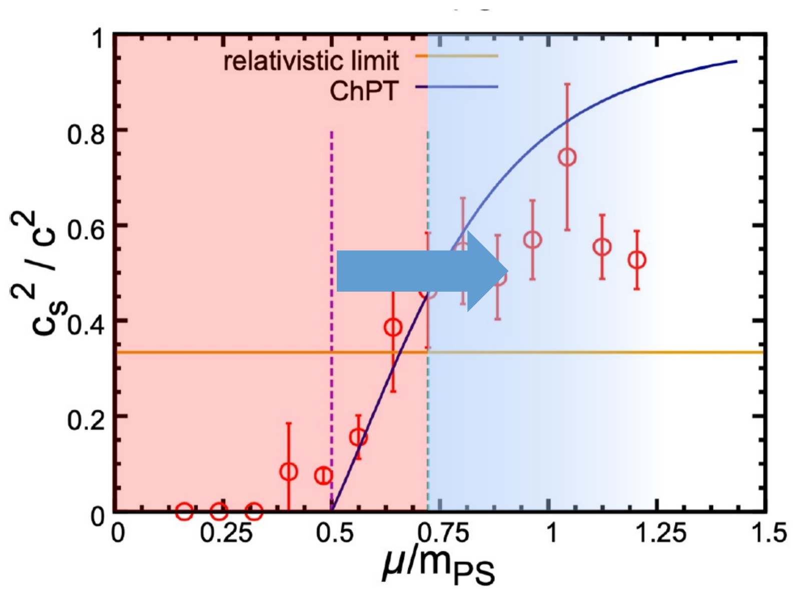

LSM result is beyond ChPT result.

$$\delta\bar{m}^2_{\sigma-\pi} \equiv \frac{m_\sigma^2 - m_\pi^2}{(\mu_q^{\rm cr})^2}$$

Sound velocity in LSM

$$\left(c_s^{\rm LSM}\right)^2 = \frac{(1 - 1/\bar{\mu}^4) + 8(\bar{\mu}^2 - 1)/\delta\bar{m}^2_{\sigma-\pi}}{(1 + 3/\bar{\mu}^4) + 8(3\bar{\mu}^2 - 1)/\delta\bar{m}^2_{\sigma-\pi}},$$

For $m_\sigma > \sqrt{3} m_\pi$,

- peak appears in c_s^2 for $\mu > m_\pi$.
- trace anomaly becomes negative.

Applicability of LSM result

M. K., D. Suenaga arXiv:2402.00430 [hep-ph]

What contributions provide peak structure?

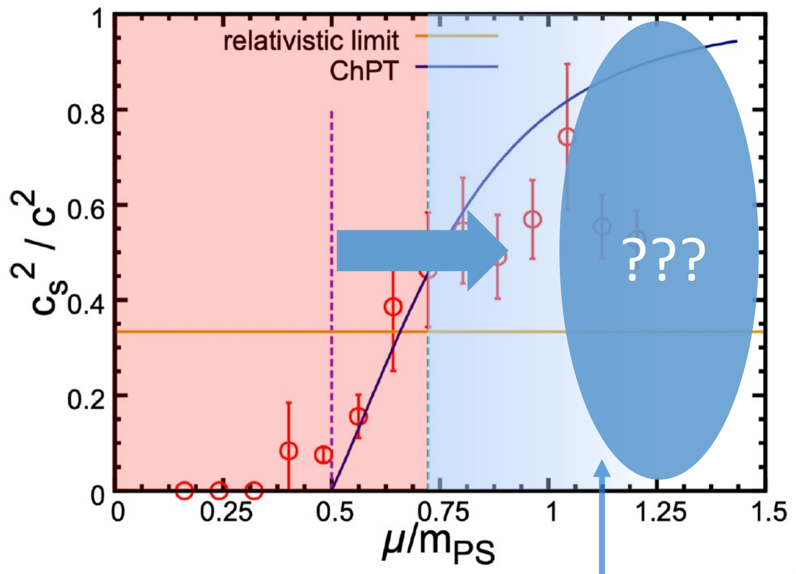

???

QC$_2$D phase structure remains unclear…

$$\delta\bar{m}^2_{\sigma-\pi} \equiv \frac{m_\sigma^2 - m_\pi^2}{(\mu_q^{\rm cr})^2}$$

Sound velocity in LSM

$$\left(c_s^{\rm LSM}\right)^2 = \frac{(1-1/\bar{\mu}^4) + 8(\bar{\mu}^2-1)/\delta\bar{m}^2_{\sigma-\pi}}{(1+3/\bar{\mu}^4) + 8(3\bar{\mu}^2-1)/\delta\bar{m}^2_{\sigma-\pi}},$$

- QC$_2$D matter keeps confined? (Son and Stephanov, 2001)
  - μ dep. of Polyakov loop is contrary to T dep..
    (e.g. Iida, Itou and Lee, 2020)
- Quark degrees of freedom appears?
  - Peak structure is induced in quark(yonic) picture.
    (e.g. McLerran and Reddy. 2019)

Applicability of LSM result

M. K., D. Suenaga arXiv:2402.00430 [hep-ph]

What contributions provide peak structure?

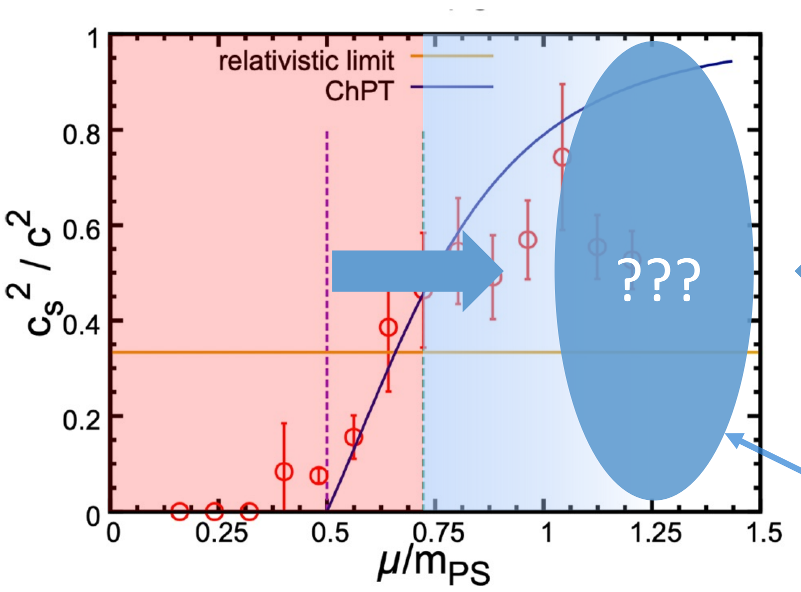

???

$$\delta\bar{m}^2_{\sigma-\pi} \equiv \frac{m_\sigma^2 - m_\pi^2}{(\mu_q^{\rm cr})^2}$$

Sound velocity in LSM

$$\left(c_s^{\rm LSM}\right)^2 = \frac{(1-1/\bar{\mu}^4) + 8(\bar{\mu}^2-1)/\delta\bar{m}^2_{\sigma-\pi}}{(1+3/\bar{\mu}^4) + 8(3\bar{\mu}^2-1)/\delta\bar{m}^2_{\sigma-\pi}},$$

μ dependence of sound velocity is still unclear…

c_s^2 approaches conformal limit from below or above?

T. Kojo, G. Baym and T. Hatsuda, Astrophys. J. 934, no.1, 46 (2022)
Y. Fujimoto and K. Fukushima, Phys. Rev. D 105, no.1, 014025 (2022)
J. Braun, A. Gei ß el and B. Schallmo, arXiv:2206.06328 [nucl-th]
L. McLerran and S. Reddy, PRL 122, no.12, 122701 (2019)

New benchmark

M. K., D. Suenaga arXiv:2402.00430 [hep-ph]

What contributions provide peak structure?

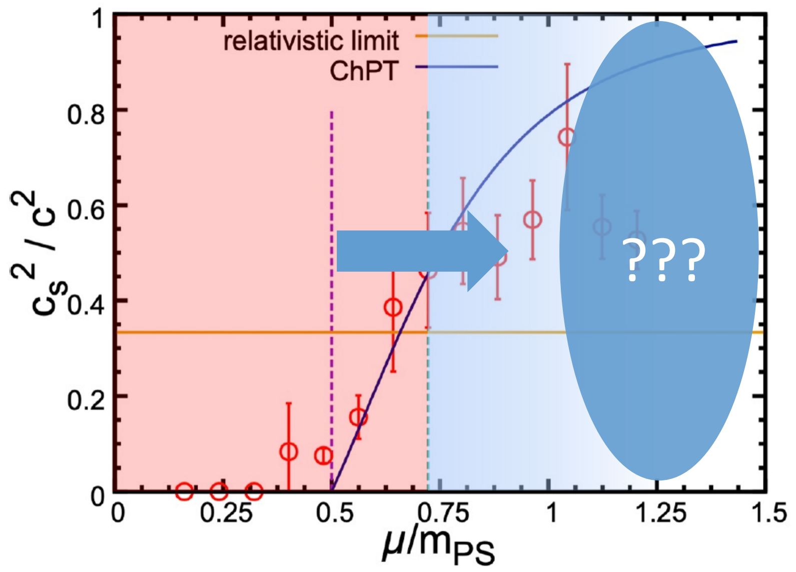

???

$$\delta \bar{m}^2_{\sigma-\pi} \equiv \frac{m_\sigma^2 - m_\pi^2}{(\mu_q^{\rm cr})^2}$$

Sound velocity in LSM

$$\left(c_s^{\rm LSM}\right)^2 = \frac{(1-1/\bar{\mu}^4) + 8(\bar{\mu}^2-1)/\delta\bar{m}^2_{\sigma-\pi}}{(1+3/\bar{\mu}^4) + 8(3\bar{\mu}^2-1)/\delta\bar{m}^2_{\sigma-\pi}},$$

Whatever its applicability…

Further investigation on

- sigma meson mass
- peak position

based on lattice simulations/other models.

Motivates…

New benchmark for understanding dense QCD matter

Thank you.